PAPER

Water-gated organic transistors on polyethylene naphthalate films

Flexible and Printed Electronics

PAPER

Water-gated organic transistors on polyethylene naphthalate films

Rafael Furlan de Oliveira[1,2,8], **Stefano Casalini**[1,9], **Tobias Cramer**[3], **Francesca Leonardi**[3,9], **Marystela Ferreira**[4], **Vincenzo Vinciguerra**[5], **Valeria Casuscelli**[6], **Neri Alves**[7], **Mauro Murgia**[3], **Luigi Occhipinti**[5,10] and **Fabio Biscarini**[1]

[1] Dipartimento di Scienze della Vita, Università di Modena & Reggio Emilia (UNIMORE), Via Campi 103, I-41125 Modena, Italy
[2] Programa de Pós-graduação em Ciência e Tecnologia de Materiais (POSMAT), Universidade Estadual Paulista (UNESP), 17033-360 Bauru, Brazil
[3] Istituto per lo Studio dei Materiali Nanostrutturati, Consiglio Nazionale delle Ricerche (ISMN-CNR), Via Gobetti n.101, I-40129 Bologna, Italy
[4] Departamento de Física, Química e Matemática (DFQM), Universidade Federal de São Carlos (UFSCar), 18052-780 Sorocaba, Brazil
[5] STMicroelectronics, Analog & MEMS Group (AMG), Str. Primosole 50, 95121 Catania, Italy
[6] STMicroelectronics, Analog & MEMS Group (AMG), Via Remo de Feo 1, 81022 Arzano (Naples), Italy
[7] Faculdade de Ciências e Tecnologia (FCT), Universidade Estadual Paulista (UNESP), 19060-900 Presidente Prudente, Brazil
[8] *Current address*: Laboratório Nacional de Nanotecnologia (LNNano), Centro Nacional de Pesquisa em Energia e Materiais (CNPEM), 13083-970 Campinas, Brazil.
[9] *Current address*: Institut de Ciéncia de Materials de Barcelona, Consejo Superior de Investigaciones Cientifica (ICMAB-CSIC), Bellaterra (Barcelona), 08193 Spain.
[10] *Current address*: University of Cambridge, Electrical Engineering Division, 9 JJ Thomson Avenue Cambridge CB3 0FA, UK.

E-mail: scasalini@icmab.es

RECEIVED
7 March 2016

REVISED
19 April 2016

ACCEPTED FOR PUBLICATION
8 May 2016

PUBLISHED
7 June 2016

Keywords: flexible electronics, organic bioelectronics, water-gated organic transistors, polyethylene naphthalate

Supplementary material for this article is available online

Abstract

Water-gated organic transistors have been successfully exploited as potentiometric transducers in a variety of sensing applications. The device response does not depend exclusively on the intrinsic properties of the active materials, as the substrate and the device interfaces play a central role. It is therefore important to fine-tune the choice of materials and layout in order to optimize the final device performance. Here, polyethylene naphthalate (PEN) has been chosen as the reference substrate to fabricate and test flexible transistors as bioelectronic transducers in liquid. PEN is a biocompatible substrate that fulfills the requirements for both bio-applications and micro-fabrication technology. Three different semiconducting or conducting polymer thin films employing pentacene, poly(3-hexylthiophene) or poly(3,4-ethylenedioxythiophene):poly(styrenesulfonate) were compared in terms of transconductance, potentiometric sensitivity and response time. The different results allow us to identify material properties crucial for the optimization of organic transistor-based transducers operating in water.

1. Introduction

Organic bioelectronics aims to develop electronic devices that can be interfaced or integrated with living matter *in vitro* and *in vivo*. A variety of applications including ultra-sensitive and highly-specific label-free biosensors [1–3], electrically-triggered drug delivery systems [4, 5], electrochemical ion pumps [6] and electronic transducers of neuronal signals has been demonstrated [7–10]. The devices are designed to fulfill the requirements of the envisioned application. Implantable devices must be minimally invasive and mechanically compliant with biological tissues [11, 12], whereas sensors need to be highly sensitive, specific, fast and standalone [1, 12–14].

Among the explored layouts, water-gated organic transistors have proven most effective in converting (bio-)chemical events into electrical signals still relying on a versatile and easy-to-standardize architectures [8, 10, 11, 15]. Two thin-film device configurations have been extensively used for biosensors: (i) electrolyte-gated organic field-effect transistors (EGOFETs) [1, 16, 17] and (ii) organic electrochemical transistors (OECTs) [8, 11]. The channel bridging source-drain electrodes patterned on a substrate consists of organic semiconductor and polymer conductor thin film,

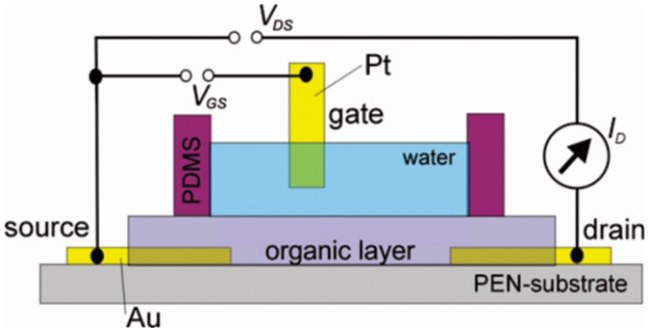

Figure 1. Schematic layout of the water-gated organic transistor. Source-drain electrodes are covered by the organic layer. A PDMS reservoir confines the aqueous solution onto the active layer.

respectively. The channel is exposed to an aqueous solution, whose electrochemical potential is set by an immersed metal gate electrode, as depicted in figure 1. The features of EGOFET and OECT that make them attractive for biomedical applications are: the large amplification of the (small) interfacial voltages, the low operational voltages, the multi-parametric response, and the straightforward integration of (bio-) recognition groups in the device [1, 5, 16].

In EGOFET, the capacitive coupling between ions in the aqueous solution and electronic charges within the organic thin-film enables the modulation of the source-drain current (I_{DS}) [12, 17]. The electrical double layer (EDL) formed at electrolyte–semiconductor interface is controlled by the gate-source voltage (V_{GS}). Due to the (sub-)nm thickness of EDL, its capacitance is in the order of tens of μF cm^{-2}, which lowers the operational voltages down to <1 V. This prevents water electrolysis and faradaic reactions [12, 17].

The EGOFET behaviour can be described by the usual organic thin-film transistor equations [14, 18]:

$$I_{DS} = \frac{W}{L} C_i \mu (V_{GS} - V_{TH}) V_{DS} \qquad V_{DS} \ll (V_{GS} - V_{TH}), \tag{1}$$

$$I_{DS} = \frac{W}{2L} C_i \mu (V_{GS} - V_{TH})^2 \qquad V_{DS} > (V_{GS} - V_{TH}). \tag{2}$$

Equations (1) and (2) describe the EGOFET response current (I_{DS}) versus voltage in linear and saturation regimes, respectively. The geometrical ratio W/L includes the channel width W and length L, C_i is the EDL capacitance per unit of area, μ is the semiconductor charge carrier mobility, V_{th} is the threshold voltage, V_{GS} and V_{DS} are the gate-source and drain-source voltages, respectively. The transconductance (g_m) is defined as:

$$g_m = \left. \frac{\partial I_{DS}}{\partial V_{GS}} \right|_{V_{DS}} \tag{3}$$

Equation (3) expresses how current is efficiently modulated by the V_{GS} at a constant V_{DS} value.

In sensing applications, changes in one or more transistor parameters (charge carrier mobility, μ, transconductance, g_m, threshold voltage, V_{TH}) are investigated as a function of a (bio-)chemical event occurring at one of the device interfaces involving gate, source, drain and the organic semiconductor in contact with the solution [12]. These functionalized interfaces endow the EGOFET with specific recognition and ultra-high sensitivity [1, 2, 16, 19]. A variety of EGOFET sensors and biosensors has been already demonstrated in literature [20–23].

OECTs have also been extensively used in bioelectronic applications [8, 11]. State-of-the-art OECTs are produced using poly(3,4-ethylenedioxythiophene):poly(styrenesulfonate) (PEDOT:PSS), a conducting polymer with high electrical conductivity (ca. 100–1000 S cm^{-1}), good chemical stability and biocompatibility [8, 24]. Potential difference between the organic layer and the electrolyte leads to a bidirectional exchange of ions between the polymer bulk and the solution to maintain the charge neutrality [13, 25]. Ion exchange is accompanied by a change of the charge carriers density, either in depletion or accumulation, along the whole volume of the organic layer [13]. The large conductivity of PEDOT:PSS results in unrivaled values of transconductance [11]. Different OECTs have been used in sensing applications [26–29] or like electronic transducers for monitoring electrocardiographic signals [11] and *in vivo* electrophysiological recordings of neuronal activity [8].

One important aspect that has been overlooked so far is the role of the substrate where the EGOFET or OECT is fabricated. The substrate should act as a bottom gate with floating potential that is determined by its chemical nature, its processing, as well as the interaction with the electrolyte solution. It is reasonable to expect that both V_{th} [16] and the capacitive coupling [30] might be sensitive to these factors. In addition, the substrate can have a fundamental impact on the morphology of the semiconducting thin film and consequently affect charge carrier mobility. This is of particular relevance for field-effect based transistors where the conducting channel forms in a thin (~1 nm) region adjacent to the dielectric.

In this work, polyethylene naphthalate (PEN) foil has been chosen as the substrate of interest to test EGOFETs and OECTs due to its biocompatibility,

flexibility, chemical inertness and transparency. In addition, PEN is widely used in organic electronics as a substrate for photolithography, high vacuum processes and solution-based coating [30–32]. Due to such a combination of attractive properties, PEN also becomes an eligible and very suitable substrate for bioelectronics applications. Limitations of PEN include its high elastic modulus (>1 GPa) meaning that only ultra-thin films will be mechanically compatible to soft biological tissue. To understand the impact of intrinsic materials properties and device design on the sensing performance of EGOFETs and OECTs, parameters such as transconductance, potentiometric sensitivity and response time were systematically evaluated. Different device architectures and geometries have been explored in order to achieve optimal transduction. This work provides valuable information about the transduction performance of different water-gated transistors necessary to consolidate biosensing platforms and in perspective overcome the present limits of potentiometric sensing.

2. Experiment

2.1. Materials and instrumentation

Pentacene, sublimated grade, ⩾99.995% trace metal basis and poly(3-hexylthiophene-2,5 diyl) (P3HT), head-to-tail regioregularity >95%, electronic grade 99.995%, were purchased from Sigma-Aldrich. Poly (3,4-ethylenedioxythiophene):poly(styrenesulfonate) (PEDOT:PSS) suspension was acquired from Clevios™. All water-gated devices were fabricated onto poly(ethylene 2,6-naphthalate) (PEN) Teonex™ Q51 plastic film purchased from DuPont Teijin Films. PEN foils (150 μm thick) were laminated on top of a 6″ blank silicon wafer, using a dual stage adhesive for thermal release of the free standing film after device fabrication, and diced in 1 × 1 cm^2 substrates. Test patterns of source and drain electrodes were designed with channel length $L = 40$ μm and width/length ratio (W/L) of 5 and 48, and with channel length $L = 10$ μm and width/length ratio (W/L) of 10, 107 and 382. The source and drain electrodes were patterned onto PEN through photolithographic processes and thin film deposition (Au/Cr). Morphological characteristics of test patterns on PEN substrate were characterized by atomic force microscopy (AFM) using an NT-MDT Smena instrument in tapping mode, and contact angle measurements (Digidrop GBX goniometer—Model D). The devices were completed by deposition of the organic layer onto the active area corresponding to the source and drain electrodes of test patterns. Electrical measurements of the device operation were carried out in a probe station with an Agilent source-meter instrument (B2912A), in ambient atmosphere.

2.2. Fabrication

The PEN test patterns were cleaned in ethanol and isopropanol under sonication for 15 min each. Pentacene-based EGOFETs were produced depositing a 10-monolayer (15 nm) pentacene film in a high vacuum chamber at a rate of 3.5 Å min^{-1} (pressure of 10^{-7} mbar). The substrate was kept at room temperature during the deposition and the film thickness was monitored by a quartz crystal microbalance inserted into the chamber.

P3HT-based EGOFETs were fabricated by spin-coating a 1 mg ml^{-1} P3HT solution in chloroform at 2000 rpm for 60 s, yielding a thickness of approximately 150 nm as determined by contact profilometry. The P3HT samples were annealed at 90 °C (in air) for 30 min to remove solvent traces.

For the OECTs fabrication, PEN test patterns were previously treated with air plasma for 3 min to improve the adhesion of spin-cast PEDOT:PSS film. The PEDOT:PSS solution containing 5% $^{v}/_{v}$ of DMSO (dimethyl sulfoxide) and 0.2% $^{v}/_{v}$ of Silquest (3-glycidoxypropyltrimethoxysilane) was used in a 3-step spin-coating process: (i) 500 rpm for 5 s, (ii) 1000 rpm for 10 s and (iii) 2000 rpm for 35 s. The samples were annealed at 50 °C for 30 min to improve their stability in water. The PEDOT:PSS film thickness was estimated as being around 100–200 nm (contact profilometry).

A polydimethylsiloxane (PDMS) reservoir was placed on top of the device to confine the electrolyte onto the active layer. A platinum wire (∅ = 1 mm) acted as a gate electrode for the electrical characterization of the devices, as shown in figure 1.

3. Results and discussion

3.1. Morphological characterization of PEN

AFM imaging was carried out for the PEN substrates before the deposition of the active material to assess the morphological properties of the biocompatible surface (figure 2). Figure 2(a) shows the presence of microscopic defects on the bare PEN. The surface roughness (root-mean-square—rms values) is 10(±3) nm on 20 × 20 μm^2 scanned areas. The roughness is approximately 6(±1) nm on smaller scan lengths deprived of defects. Figure 2(b) shows the AFM image of an interdigitated electrode and its step profile. The electrode height is 55 nm (figure 2(b) inset). The same features observed on the bare PEN are transferred to the electrode surface that exhibits 11(±2) nm rms roughness.

PEN exhibits water contact angles centered at 80°, in agreement with reported data [31]. As previously described (see experimental section), plasma treatment yields robust adhesion of water-based PEDOT:PSS on PEN substrate.

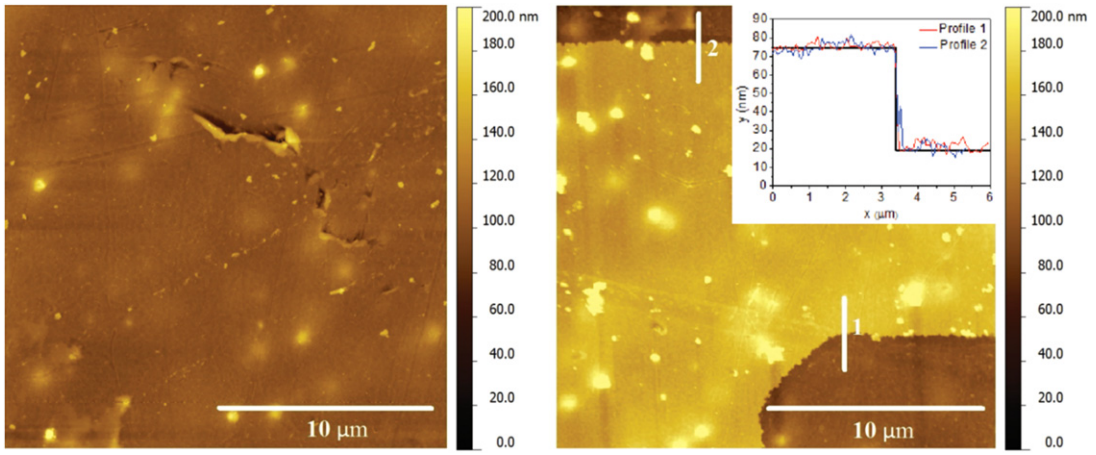

Figure 2. On the left, AFM image of a bare test pattern showing the morphology of the PEN substrate. On the right, an image of the source-drain electrode. Inset: electrode height profile.

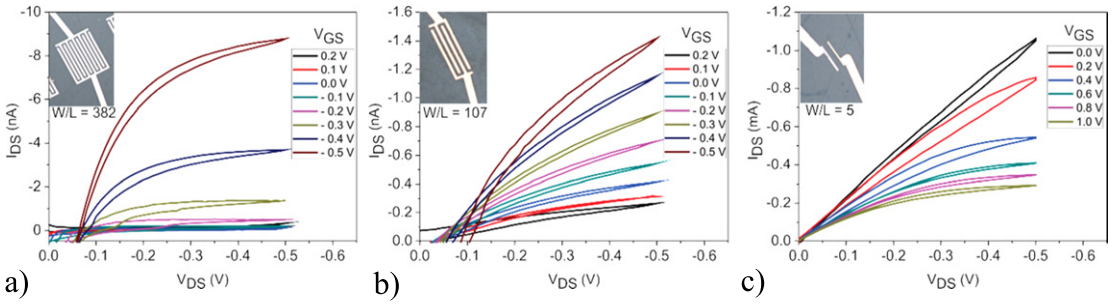

Figure 3. *I–V* output characteristics of water-gated organic transistors based on pentacene (a), P3HT (b) and PEDOT:PSS (c). Inset of each panel shows the source-drain electrode geometry.

3.2. Electrical characterization of water-gated organic transistors

The electrical measurements of pentacene and P3HT-based EGOFETs were recorded in deionized water (DI) whereas the OECT was measured in 100 mM NaCl solution due to its working principle. The *I–V* output characteristics (I_{DS} versus V_{DS}) of our devices were acquired by sweeping the drain-source voltage (V_{DS}) from 0.0 V to −0.5 V at different V_{GS}, as depicted in figure 3. *I–V* transfer characteristics related to EGOFETs (I_{DS} versus V_{GS}) were obtained varying V_{GS} from 0.2 V to −0.5 V at constant $V_{DS} = -0.5$ V (supplementary figure S1). On the other hand, *I–V* transfer characteristics of OECT were carried out sweeping V_{GS} from 0.0 V to 1.0 V at $V_{DS} = -1.0$ V (figure S1). These small working potentials are suitable for the device operation in aqueous solutions to avoid water electrolysis and undesired faradaic reactions that might degrade the organic layer [12]. Important device parameters such as g_m, μ and V_{th} are extracted from transfer curves, as described elsewhere [14].

The EGOFET and OECT output characteristics (figure 3) exhibit the typical transistor response at low-voltage operation for all fabricated devices. In particular, pentacene EGOFETs showed well-defined saturation plateaus in the whole V_{GS} range (figure 3(a)). The operation of pentacene-based devices required the use of source-drain electrodes with the highest W/L ratio (e.g. 382), as shown in the inset, to yield recordable I_{DS}. As a result, we obtained devices with μ around 5.9×10^{-5} cm^2 V^{-1} s^{-1} by assuming the electrical double layer capacitance for the water/pentacene interface as 7–8.5 μF cm^{-2} [32]. The extracted V_{th} exhibits values around −0.21 V while the device transconductance was evaluated as being approximately 0.012 ± 0.002 μS.

Figure 3(b) shows the *I–V* output characteristics of the P3HT-based EGOFET. These devices provided recordable currents even using lower geometrical ratio, namely $W/L = 107$, compared to pentacene-based ones. From the electrical characteristics of P3HT-based EGOFETs, mobility values of approximately $\mu = 2 \times 10^{-5}$ cm^2 V^{-1} s^{-1}, by considering $C_{EDL} = 3$–6 μF cm^{-2} for P3HT/water interface [17], V_{TH} around 0.28 V and $g_m = 0.003 \pm 0.0001$ μS were extracted.

Both pentacene- and P3HT-based EGOFETs exhibited limited but finite hysteresis and contact

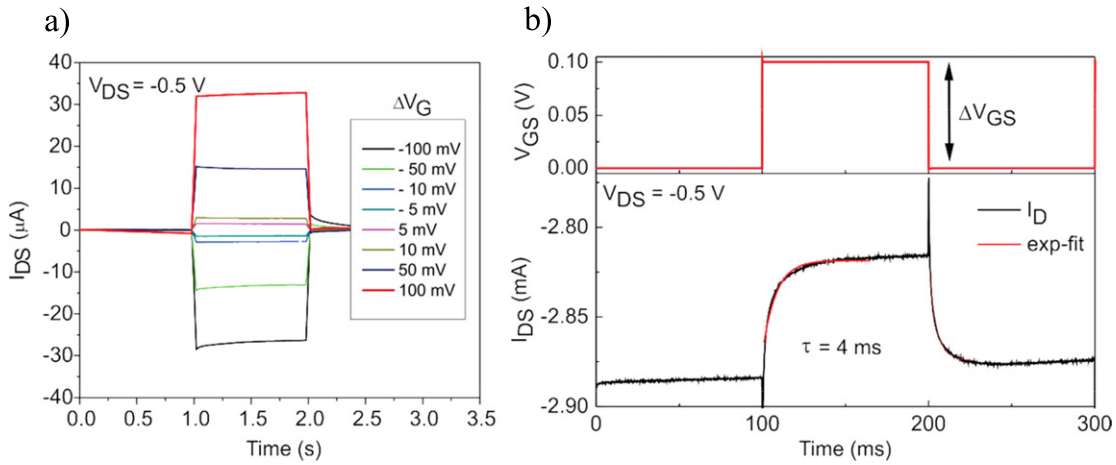

Figure 4. (a) Potentiometric sensing experiment showing high sensibility of I_{DS} to small gate potential variations (ΔV_G) for a PEDOT:PSS OECT ($V_{DS} = -0.5$ V). (b) Operational speed plot for a PEDOT:PSS OECT showing estimated switching times approximately 4 ms ($V_{DS} = -0.5$ V).

resistances (figures 3(a) and (b)). The small hysteresis commonly observed for EGOFETs is attributed to the EDL formation, which depends on (i) ionic strength of the aqueous solution, (ii) morphology and other intrinsic properties of the active thin-film, (iii) type of metal and area of the gate electrode [17, 33]. No electrochemical doping occurs in either pentacene or P3HT devices due to the low leakage gate currents (below 5 nA) observed and the absence of electrochemical redox peaks on these curves (see figure S2). Therefore, the charge accumulation within the pentacene and P3HT-based conductive channels is mainly due to the capacitive coupling of the EDL ions and the organic semiconductor charge carriers.

Figure 3(c) illustrates the output curve of the OECT. OECTs operate in depletion mode and charge modulation is due to electrochemical de-doping of the conducting polymer. When V_{GS} bias is not applied, the OECT responds as a conductor, whereas semiconductor behavior takes place when V_{GS} is positively biased. The intrinsic conductivity of PEDOT:PSS is sufficiently high to provide substantial electrical currents (in the mA range) even using electrodes with the lowest available W/L ratio (namely, equal to 5), as well as to overcome possible contact resistance effects related to the imperfections on the PEN surface. From the electrical characteristics of OECT, g_m values as high as 2000 ± 300 μS were determined. These values are typically much higher than g_m calculated for EGOFETs.

3.3. Potentiometric sensitivity and response time

The potentiometric sensitivity of the studied devices was probed by applying small gate voltage modulation (ΔV_{GS}) for constant source-drain voltage ($V_{DS} = -0.5$ V) during a fixed time interval. Figure 4(a) shows the resulting drain current changes of a PEDOT:PSS OECT after polynomial treatment for current drift correction. These devices showed reasonable sensitivity to small potential fluctuations (limit down to 5 mV) with signal-to-noise (S/N) ratios of approximately 100, as calculated for $|\Delta V_{GS} = 10$ mV|. The ability of water-gated devices to sense small potential variations (from hundreds of μV to a few mV) with high S/N ratios is important, for example, in the transduction of transmembrane action potentials of neuronal cells [35]. This type of application also requires fast operational speeds, since action potentials have a timescale of milliseconds [34]. A switching time of $\tau = 4$ ms was estimated for the PEDOT:PSS device by fitting a first order exponential decay curve, as depicted in figure 4(b). The integration time for extracting the switching speeds of water-gated transistors was set as <1 ms. Pentacene EGOFETs demonstrated better sensitivity (approximately doubled S/N ratios) compared to PEDOT:PSS-based OECTs, but switching speeds 3–5 times slower (figure S3). P3HT EGOFETs exhibited the poorest sensitivity among the tested devices (S/N ratio of 4.5) with the slowest switching speeds. The respective curves for the EGOFETs are described in the supporting information (figures S3 and S4). All the parameters that characterize the potentiometric response of the tested devices are summarized in table 1.

Table 1. Operational parameters for different water-gated organic transistors.

	g_m (μS)	S/N[a]	τ (ms)
Pentacene	0.012 ± 0.002	194	10–20
P3HT	0.003 ± 0.0001	4.5	>100
PEDOT:PSS	2000 ± 300	111	4

[a] S/N calculated for $|\Delta V_{GS}| = 10$ mV.

Although P3HT and pentacene EGOFETs have shown comparable g_m and μ values, the potentiometric performance of pentacene devices (S/N ratio and τ) is much better than that of the P3HT ones. The

potentiometric sensitivity of pentacene EGOFETs is comparable to that of the PEDOT:PSS OECT which exhibited g_m values 10^5 times higher than pentacene EGOFETs even using lower electrode interdigitation. A higher g_m allows one to achieve more effective amplification of the event of interest during a sensing experiment. However, OECTs work in depletion and have a large background current due to the high charge carrier densities which ultimately reduces the signal-to-noise ratio and puts it at a similar scale to the pentacene EGOFET. PEDOT:PSS OECTs showed switching times consistent to those reported in the literature ($\tau = 1.5$ ms) [11], whereas pentacene EGOFETs showed slightly slower switching speeds than the devices reported by Cramer *et al* fabricated onto Si/SiO_2 substrates ($\tau = 4.6$ ms) [34]. OECTs exhibited the fastest response speed, although it was found that the slow diffusion of the ions in the organic bulk film could be limiting [12]. However, recent findings have shown that ion transport in hydrated PEDOT:PSS is almost comparable to transport through water [36]. In addition, OECTs show a much higher electronic conduction than EGOFETs due to the larger charge densities therefore reducing the resistance in the RC-circuit that governs the temporal response.

Comparing the performance of the three devices, we find a significant impact of the PEN substrate on the properties of the EGOFETs. Both the small molecule semiconductor (pentacene) and polymeric semiconductor (P3HT) showed a strong reduction in transport properties leading to a decrease of the charge mobility by some orders of magnitude when compared to reference devices prepared on flat SiO_2 substrates. The deterioration is attributed to the increased surface roughness of PEN in combination with the increasing of hydrophobic properties. As a consequence, we hypothesize that the ordered thin film morphology of pentacene or P3HT cannot be established on PEN substrates. Strong morphology disorder is of particular relevance for field-effect based devices as the conducting channel is confined to an ultra-thin region (<1 nm) adjacent to the liquid interface. Any barrier in this region emerging, for example, from surface roughness exceeding 10 nm will strongly block transport. In contrast, OECT devices exploit the whole volume of the semiconducting film for carrier transport and consequently they more effectively conserve transducer properties even when fabricated on PEN. Finally, we believe the results found here can be extrapolated to other plastic substrates presenting similar roughness values and surface defects.

4. Conclusions

Water-gated organic transistors based on pentacene, P3HT and PEDOT:PSS were fabricated on PEN substrates and their electrical behavior is described. Attention has been mainly paid to the correlation between materials properties, device architecture and transduction ability of these devices. Despite some interesting characteristics presented by PEN substrates for bioelectronic applications (e.g. flexibility, chemical inertness, transparency, compatibility with photolithographic processes), the surface defects are the limiting factor for EGOFET configuration regardless of the organic semiconductor used. As a result, pentacene- and P3HT-based EGOFETs exhibited mobility values around 5.9×10^{-5} and 2×10^{-5} cm^2 V^{-1} s^{-1}, respectively, which are lower than other devices fabricated on other substrates. On the other hand, OECTs have shown better electrical performances than EGOFETs such as (i) higher g_m values (~2000 μS), (ii) better potentiometric sensitivity (S/N ratios >100) and faster response ($\tau \sim 4$ ms). These characteristics are essential for applications as bioelectronics sensors. This highlights how the PEDOT:PSS layer is robust when used on flexible biocompatible substrates even in the presence of surface morphology with relatively large roughness.

Acknowledgments

This work was funded by the EU 7th Framework Programme [FP7/2007-2013] under Grant Agreement No. 280772, Implantable Organic Nanoelectronics (iONE-FP7) project. We are grateful to FAPESP (Brazil) for additional financial support to R.F.O. (Proc. 2013/03857-0 and Proc. 2011/00229-2).

References

[1] Casalini S, Leonardi F, Cramer T and Biscarini F 2013 Organic field-effect transistor for label-free dopamine sensing *Org. Electron.* **14** 156–63
[2] Buth F, Donner A, Sachsenhauser M, Stutzmann M and Garrido J A 2012 Biofunctional electrolyte-gated organic field-effect transistors *Adv. Mater.* **24** 4511–7
[3] Khan H U, Jang J, Kim J-J and Knoll W 2011 *In situ* antibody detection and charge discrimination using aqueous stable pentacene transistor biosensors *J. Am. Chem. Soc.* **133** 2170–6
[4] Yue Z, Moulton S E, Cook M, O'Leary S and Wallace G G 2013 Controlled delivery for neuro-bionic devices *Adv. Drug Deliv. Rev.* **65** 559–69
[5] Foschi G, Leonardi F, Scala A, Biscarini F, Kovtun A, Liscio A, Mazzaglia A and Casalini S 2015 Electrical release of dopamine and levodopa mediated by amphiphilic β-cyclodextrins immobilized on polycrystalline gold *Nanoscale* **7** 20025–32
[6] Isaksson J, Kjäll P, Nilsson D, Robinson N, Berggren M and Richter-Dahlfors A 2007 Electronic control of Ca2+ signalling in neuronal cells using an organic electronic ion pump *Nat. Mater.* **6** 673–9
[7] Furukawa Y, Shimada A, Kato K, Iwata H and Torimitsu K 2013 Monitoring neural stem cell differentiation using PEDOT–PSS based MEA *Biochim. Biophys. Acta* **1830** 4329–33
[8] Khodagholy D *et al* 2013 *In vivo* recordings of brain activity using organic transistors *Nat. Commun.* **4** 1575
[9] Von Holst H 2013 Organic bioelectrodes in clinical neurosurgery *Biochim. Biophys. Acta* **1830** 4345–52
[10] Cramer T, Chelli B, Murgia M, Barbalinardo M, Bystrenova E, de Leeuw D M and Biscarini F 2013 Organic ultra-thin film transistors with a liquid gate for extracellular stimulation and

recording of electric activity of stem cell-derived neuronal networks *Phys. Chem. Chem. Phys.* **15** 3897
[11] Campana A, Cramer T, Simon D T, Berggren M and Biscarini F 2014 Electrocardiographic recording with conformable organic electrochemical transistor fabricated on resorbable bioscaffold *Adv. Mater.* **26** 3874–8
[12] Cramer T, Campana A, Leonardi F, Casalini S, Kyndiah A, Murgia M and Biscarini F 2013 Water-gated organic field effect transistors—opportunities for biochemical sensing and extracellular signal transduction *J. Mater. Chem.* B **1** 3728
[13] Tarabella G, Mahvash Mohammadi F, Coppedè N, Barbero F, Iannotta S, Santato C and Cicoira F 2013 New opportunities for organic electronics and bioelectronics: ions in action *Chem. Sci.* **4** 1395
[14] Torsi L, Magliulo M, Manoli K and Palazzo G 2013 Organic field-effect transistor sensors: a tutorial review *Chem. Soc. Rev.* **42** 8612
[15] De Oliveira R F, Merces L, Vello T P and Bof Bufon C C 2016 Water-gated phthalocyanine transistors: operation and transduction of the peptide–enzyme interaction *Org. Electron.* **31** 217–26
[16] Casalini S, Dumitru A C, Leonardi F, Bortolotti C A, Herruzo E T, Campana A, de Oliveira R F, Cramer T, Garcia R and Biscarini F 2015 Multiscale sensing of antibody–antigen interactions by organic transistors and single-molecule force spectroscopy *ACS Nano* **9** 5051–62
[17] Kergoat L, Herlogsson L, Braga D, Piro B, Pham M-C, Crispin X, Berggren M and Horowitz G 2010 A water-gate organic field-effect transistor *Adv. Mater.* **22** 2565–9
[18] Kim C-H, Bonnassieux Y and Horowitz G 2014 Compact DC modeling of organic field-effect transistors: review and perspectives *IEEE Trans. Electron Devices* **61** 278–87
[19] Leonardi F, Casalini S, Albonetti C and Biscarini F 2015 Charge-injection organic gauges to detect dopamine down to the nanomolar scale *IEEE Trans. Electron Devices* **62** 4251–7
[20] Magliulo M, Mallardi A, Mulla M Y, Cotrone S, Pistillo B R, Favia P, Vikholm-Lundin I, Palazzo G and Torsi L 2013 Electrolyte-gated organic field-effect transistor sensors based on supported biotinylated phospholipid bilayer *Adv. Mater.* **25** 2090–4
[21] Suspène C, Piro B, Reisberg S, Pham M-C, Toss H, Berggren M, Yassar A and Horowitz G 2013 Copolythiophene-based water-gated organic field-effect transistors for biosensing *J. Mater. Chem.* B **1** 2090
[22] Schmoltner K, Kofler J, Klug A and List-Kratochvil E J W 2013 Electrolyte-gated organic field-effect transistor for selective reversible ion detection *Adv. Mater.* **25** 6895–9
[23] Mulla M Y, Tuccori E, Magliulo M, Lattanzi G, Palazzo G, Persaud K and Torsi L 2015 Capacitance-modulated transistor detects odorant binding protein chiral interactions *Nat. Commun.* **6** 6010
[24] Khodagholy D, Gurfinkel M, Stavrinidou E, Leleux P, Herve T, Sanaur S and Malliaras G G 2011 High speed and high density organic electrochemical transistor arrays *Appl. Phys. Lett.* **99** 163304
[25] Liao C and Yan F 2013 Organic semiconductors in organic thin-film transistor-based chemical and biological sensors *Polym. Rev.* **53** 352–406
[26] Lin P, Luo X, Hsing I-M and Yan F 2011 Organic electrochemical transistors integrated in flexible microfluidic systems and used for label-free DNA sensing *Adv. Mater.* **23** 4035–40
[27] Lin P, Yan F, Yu J, Chan H L W and Yang M 2010 The application of organic electrochemical transistors in cell-based biosensors *Adv. Mater.* **22** 3655–60
[28] Sessolo M, Rivnay J, Bandiello E, Malliaras G G and Bolink H J 2014 Ion-selective organic electrochemical transistors *Adv. Mater.* **26** 4803–7
[29] He R-X, Zhang M, Tan F, Leung P H M, Zhao X-Z, Chan H L W, Yang M and Yan F 2012 Detection of bacteria with organic electrochemical transistors *J. Mater. Chem.* **22** 22072
[30] Palazzo G, De Tullio D, Magliulo M, Mallardi A, Intranuovo F, Mulla M-Y, Favia P, Vikholm-Lundin I and Torsi L 2014 Detection beyond debye's length with an electrolyte-gated organic field-effect transistor *Adv. Mater.* **27** 911–6
[31] Klauk H, Zschieschang U, Pflaum J and Halik M 2007 Ultralow-power organic complementary circuits *Nature* **445** 745–8
[32] Simon D, Ware T, Marcotte R, Lund B R, Smith D W, Di Prima M, Rennaker R L and Voit W 2013 A comparison of polymer substrates for photolithographic processing of flexible bioelectronics *Biomed. Microdevices* **15** 925–39
[33] Kormunda M, Homola T, Matousek J, Kovacik D, Cernak M and Pavlik J 2012 Surface analysis of poly(ethylene naphthalate) (PEN) films treated at atmospheric pressure using diffuse coplanar surface barrier discharge in air and in nitrogen *Polym. Degrad. Stab.* **97** 547–53
[34] Cramer T, Kyndiah A, Murgia M, Leonardi F, Casalini S and Biscarini F 2012 Double layer capacitance measured by organic field effect transistor operated in water *Appl. Phys. Lett.* **100** 143302
[35] Fromherz P 2006 Three levels of neuroelectronic interfacing: silicon chips with ion channels, nerve cells, and brain tissue *Ann. NY Acad. Sci.* **1093** 143–60
[36] Stavrinidou E, Leleux P, Rajaona H, Khodagholy D, Rivnay J, Lindau M, Sanaur S and Malliaras G G 2013 Direct measurement of ion mobility in a conducting polymer *Adv. Mater.* **25** 4488–93